Applied Mathematics and Computational Intelligence
Volume 8, No.1, Dec 2019 [17-30]

Effect of Suction on the Stagnation Point Flow and Heat Transfer over a Stretching/Shrinking Sheet in a Porous Medium with Stability Analysis

Noormaizatulnazuha Mohamad[1*], Fatinnabila Kamal[1] and Khairy Zaimi[1]

[1]*Institute of Engineering Mathematics, Universiti Malaysia Perlis, Pauh Putra Campus, 02600 Arau, Perlis, Malaysia.*

ABSTRACT

This research investigates the problem of stagnation point flow and heat transfer over a stretching/shrinking sheet past a porous medium with suction effect. Firstly, the mathematical model that governed the fluid flow and heat transfer were formulated. Then, the governing nonlinear partial differential equations were transformed into ordinary differential equations using similarity transformation. The system of ordinary differential equations is then solved numerically using bvp4c function in Matlab software. The effect of suction on the skin friction coefficient and the local Nusselt number, as well as the velocity and temperature profiles, are obtained and analysed. The numerical result obtained is presented in the form of graphs and tables. The dual solutions are obtained for a certain range of parameters. The stability analysis has been performed and the result shows that the upper branch solution is stable while the lower branch solution is unstable.

Keywords: Stagnation Point Flow, Stretching/Shrinking Sheet, Suction Effect, Dual Solution.

1. INTRODUCTION

A few decades ago, the study of flow near a stagnation point has grabbed much attention due to its wide range of application in many industrial manufacturing processes. Hiemenz [1] is the first person who has studied the two-dimensional stagnation point flow. In his study, the thickness of the boundary layer is constant and the distance from the stagnation point is proportional to the velocity in the outer flow. The Navier-Stokes equation was reduced to the ordinary differential equation by Hiemenz as stated by Abbas et al. [2].

The study done by Hiemenz [1] was extended by Crane [3] because Hiemenz is the first person who pioneered the study of flow over a stretching sheet by solving the steady two-dimensional flow past a linearly stretching sheet. The velocity is varying linearly with the distance from a fixed point, hence the study by Crane [3] focus on the steady boundary layer flow of an incompressible viscous liquid caused by the linear stretching of an elastic flat sheet. After that, Gupta and Gupta [4] extended the study by adding suction or blowing effect and they found that the stretching surface is not necessarily continuous.

The study of suction on the boundary layer flow has important application in the fields of aerodynamics and space science. The unsteady magnetohydrodynamic (MHD) flow and heat transfer over a stretching permeable surface with suction or injection have been investigated by Choudhary et al. [5]. They found that the rate of heat transfer, temperature profile and velocity profile were affected by the suction or injection effect.

*Corresponding Author: *noormaizatulnazuhamohamad@gmail.com*

The study of MHD flow towards a permeable stretching/shrinking sheet of a nanofluid with the addition of suction/injection was done by Naramgari and Sulochana [6]. They analysed the influence of chemical reaction and thermal radiation and solved the problem numerically by using bvp4c function in Matlab. The study found the existence of dual solutions for a certain range of stretching/shrinking and suction/injection parameter. The radiation parameter helps enhance the temperature profile and decrease the concentration profiles as well as the rate of heat transfer. From this study, the rate of heat transfer, flow, and friction factor in stretching surface were reduced by the magnetic field parameter.

Motivated by the studies mentioned above, the objective of the present studies is to investigate the effect of suction on stagnation point flow and heat transfer over a stretching/shrinking sheet past a porous medium. This study is the extension from Rosali and Ishak [7], by adding the suction effect as well as the stability analysis. The effects of the suction parameter are discovered and explained in detail. The dual solutions are expected to exist for this problem. Temporal stability analysis was conducted to verify which solution is stable and has a real physical implication.

2. MATHEMATICAL FORMULATION

Consider a steady two-dimensional stagnation-point flow over a stretching/shrinking sheet. The coordinate system where x-axis along the stretching/shrinking surface, while the y-axis is measured normal to it was denoted. It is assumed that the velocity of the stretching/shrinking sheet is $U_w = ax$, where $a > 0$ corresponds to stretching sheet and $a < 0$ is for the shrinking case, while the velocity of the external flow is given by $U_\infty = cx$, where $c > 0$ is the strength of stagnation flow. The temperature of the surface is $T_w(x) = T_\infty + bx$, where b is a constant and T_∞ is the temperature of the ambient fluid. The flow configuration and the coordinate system are presented in Figure 1. Under above boundary layer approximation assumptions, the governing equation for conservation of mass, momentum equation and energy equations of this problem can be expressed as the following (see Rosali & Ishak [7]; Ishak et al. [8]):

$$\frac{\partial u}{\partial x} + \frac{\partial v}{\partial y} = 0 \tag{1}$$

$$u\frac{\partial u}{\partial x} + v\frac{\partial u}{\partial y} = U_\infty \frac{dU_\infty}{dx} + \nu\frac{\partial^2 u}{\partial y^2} + \frac{\nu}{K_1}(U_\infty - u) \tag{2}$$

$$u\frac{\partial T}{\partial x} + v\frac{\partial T}{\partial y} = \alpha\frac{\partial^2 T}{\partial y^2} \tag{3}$$

where x and y represent the coordinate axes along the moving sheet and normal to it with respect to the origin at the stagnation point. u and v are velocity component along the x-axis and y-axis respectively, T is the fluid temperature, K_1 is the permeability of porous medium, α is the thermal diffusivity, and ν is the kinematic viscosity.

The appropriate boundary conditions are:

$$u = U_w(x) = ax, v = V_w, T = T_w \quad \text{at} \quad y = 0,$$
$$u \to U_\infty(x) = cx, T = T_\infty \quad \text{as} \quad y \to \infty, \tag{4}$$

where u and v are velocity component in the x and y direction, a and c are positive constant, T is the fluid temperature, and V_w is the mass velocity with $V_w > 0$ for suction.

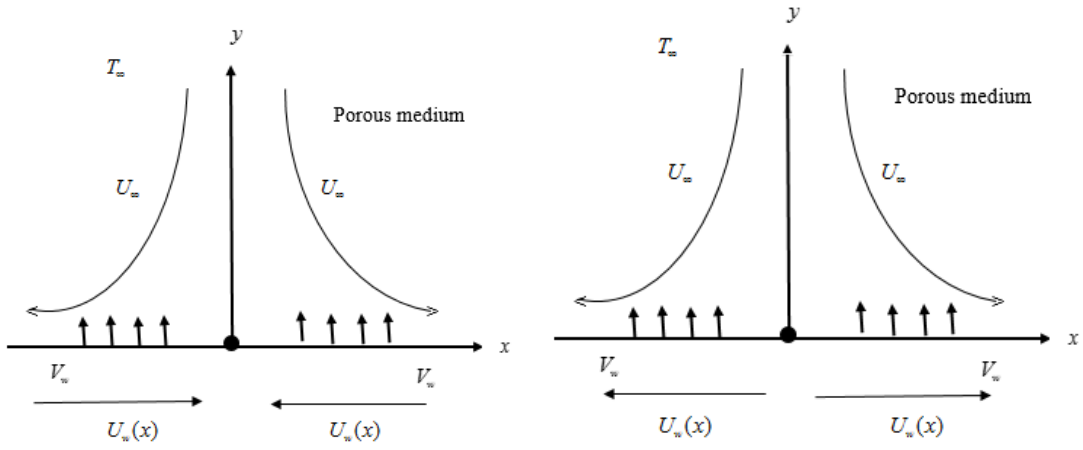

` a) Shrinking case with , $a < 0$ b) Stretching case with , $a > 0$

Figure 1. Physical model and coordinate system.

3. SIMILARITY TRANSFORMATIONS

In order to obtain the similarity solutions for equations (1)-(3) with boundary condition (4), we have introduced the following similarity variables of the following form (see Rosali & Ishak [7]):

$$\psi = (axU_\infty)^{\frac{1}{2}} f(\eta), \qquad \eta = \left(\frac{U_\infty x}{\alpha}\right)^{\frac{1}{2}} \frac{y}{x}, \quad \theta(\eta) = \frac{T - T_\infty}{T_w - T_\infty} \quad , \tag{5}$$

where ψ is the stream function, which is defined as in Equation (6)(see Rosali & Ishak [7]):

$$u = \frac{\partial \psi}{\partial y}, \qquad v = -\frac{\partial \psi}{\partial x} \, . \tag{6}$$

Then, substituting equations (5)-(6) into equations (2)-(3) while equation (3.1) is identically satisfied, we get

$$\Pr f''' + ff'' + 1 - \left[f'\right]^2 + K\left[1 - f'\right] = 0 \, , \tag{7}$$

$$\theta'' + f\theta' - f'\theta = 0 \, . \tag{8}$$

The boundary conditions (4) become:

$$f'(0) = \varepsilon, f(0) = \gamma, \theta(0) = 1 \, ,$$
$$\theta(0) = 1, \theta(\eta) \to 0 \text{ as } \eta \to \infty \, . \tag{9}$$

where $\Pr = \frac{\nu}{\alpha}$ is the Prandtl number, $K = \frac{\nu}{cK_1}$ is the permeability parameter, $\gamma > 0$ is the suction parameter, and $\varepsilon = a/c$ is the stretching/shrinking parameter with $\varepsilon > 0$ for a stretching sheet and $\varepsilon < 0$ for a stretching sheet.

The physical quantities of interest in this study are the skin friction coefficient C_f and the local Nusselt number Nu_x as stated by Rosali & Ishak [7] which are defined as:

$$C_f = \frac{\tau_w}{\rho U_\infty^{\,2} / 2}, \qquad Nu_x = \frac{x q_w}{k(T_w - T_\infty)} \tag{10}$$

Here, ρ is the fluid density, τ_w and q_w are the surface shear stress and surface heat flux, respectively are given by

$$\tau_w = \mu \left(\frac{\partial u}{\partial y} \right)_{y=0}, \qquad q_w = -k \left(\frac{\partial T}{\partial y} \right)_{y=0} \tag{11}$$

where μ and k are the dynamic viscosity and thermal conductivity respectively. Substituting equation (11) into equation (10) and using equations (5) and (6), we get:

$$\frac{1}{2} C_f \, \mathrm{Re}_x^{\frac{1}{2}} \mathrm{Pr}^{-\frac{1}{2}} = f''(0), \qquad Nu_x Pe_x^{-\frac{1}{2}} = -\theta'(0), \tag{12}$$

where the local Reynolds number and the Peclet number are defined as:

$$\mathrm{Re}_x = \frac{U_\infty x}{\mu} \qquad \text{and} \qquad Pe_x = \frac{U_\infty x}{\alpha} \tag{13}$$

4. STABILITY ANALYSIS

Recently, stability analysis has become a trend between researchers in order to verify the stability of the dual solutions. The idea of stability analysis is to verify the significance of dual solutions was started by Merkin [9]. As stated by Weidman et al. [10], in order to study the stability of the dual solutions, the unsteady state flow case need to be considered. There is a lot of researchers that utilise the stability analysis in their studies such as Awaludin et al. [11], Jahan et al. [12], and Ismail et al. [13].

Consider the problem of unsteady. Equation (1) holds while equations (2)-(3) are replaced by:

$$\frac{\partial u}{\partial t} + u\frac{\partial u}{\partial x} + v\frac{\partial u}{\partial y} = U_\infty \frac{dU_\infty}{dx} + \nu \frac{\partial^2 u}{\partial y^2} + \frac{\nu}{K_1}(U_\infty - u), \tag{14}$$

$$\frac{\partial T}{\partial t} + u\frac{\partial T}{\partial x} + v\frac{\partial T}{\partial y} = \alpha \frac{\partial^2 T}{\partial y^2}. \tag{15}$$

We introduce new similarity variables as follows:

$$\psi = (\alpha x U_\infty)^{\frac{1}{2}} f(\eta, \tau), \quad \eta = \left(\frac{U_\infty x}{\alpha} \right)^{\frac{1}{2}} \frac{y}{x}, \quad \theta(\eta, \tau) = \frac{T - T_\infty}{T_w - T_\infty}, \quad \tau = ct. \tag{16}$$

We introduce the dimensionless time variable τ that will follow the definition of u and v.

$$u = cxf'(\eta,\tau), \qquad v = -\sqrt{c\alpha} f(\eta,\tau). \tag{17}$$

Using equations (16)-(17) into (14)-(15), the following equations are obtained:

$$\Pr\frac{\partial^3 f}{\partial\eta^3} + f\frac{\partial^2 f}{\partial\eta^2} + 1 - \left(\frac{\partial f}{\partial\eta}\right)^2 + K\left[1 - \frac{\partial f}{\partial\eta}\right] - \frac{\partial^2 f}{\partial\eta\partial\tau} = 0 \tag{18}$$

$$\frac{\partial^2\theta}{\partial\eta^2} + f\frac{\partial\theta}{\partial\eta} - \theta\frac{\partial f}{\partial\eta} - \frac{\partial\theta}{\partial\tau} = 0. \tag{19}$$

Thus, the boundary conditions become:

$$\frac{\partial f}{\partial\eta}(0,\tau) = \varepsilon, f(0,\tau) = \gamma, \theta(0,\tau) = 1,$$
$$f'(\eta,\tau) \to 1, \theta(\eta,\tau) \to 0 \text{ as } \eta \to \infty. \tag{20}$$

In order to test the stability behaviour, the basic flow $f = f_0(\eta)$ and $\theta = \theta_0(\eta)$ which satisfy the equations (7)-(8) subject to boundary conditions (9) will be perturbed with disturbance as stated by Weidman et al. [10].

$$f(\eta,\tau) = f_0(\eta) + e^{-\lambda\tau}F(\eta,\tau),$$
$$\theta(\eta,\tau) = \theta_0(\eta) + e^{-\lambda\tau}G(\eta,\tau), \tag{21}$$

where λ is an unknown eigenvalue, and $F(\eta,\tau)$ and $G(\eta,\tau)$ are functions. Solutions of the eigenvalue problem (16)-(18) give an infinite set of eigenvalues $\lambda_1 < \lambda_2 < \lambda_3 < \ldots$; λ_1, If λ_1 is negative, there is an initial growth of disturbances and the flow is unstable, but when λ_1 is positive, there is an initial decay and the flow is stable. Substituting (21) into equations (18)-(19), the following equations were obtained:

$$\Pr\frac{\partial^3 F}{\partial\eta^3} + f_0\frac{\partial^2 F}{\partial\eta^2} + f''_0 F - \left[2f'_0 + K - \lambda\right]\frac{\partial F}{\partial\eta} - \frac{\partial^2 F}{\partial\eta\partial\tau} = 0, \tag{22}$$

$$\frac{\partial^2 G}{\partial\eta^2} + f_0\frac{\partial G}{\partial\eta} + \theta'_0 F - \theta_0\frac{\partial F}{\partial\eta} - f'_0 G + \lambda\frac{\partial G}{\partial\eta} - \frac{\partial G}{\partial\tau} = 0, \tag{23}$$

along the boundary conditions:

$$\frac{\partial}{\partial\eta}F(0,\tau) = 0, F(0,\tau) = 0, G(0,\tau) = 0, \tag{24}$$

$$\frac{\partial}{\partial\eta}F(\eta,\tau) \to 0, G(\eta,\tau) \to 0 \text{ as } \eta \to \infty. \tag{25}$$

The solutions $f(\eta) = f_0(\eta)$ and $\theta(\eta) = \theta_0(\eta)$ of the steady equations (7) and (8) are obtained by setting $\tau = 0$. Hence, $F = F_0(\eta)$ and $G = G_0(\eta)$ in (22) and (23) identify the initial growth or decay of the solution (21). Equations (22) and (23) become the following linear eigenvalue problem

$$\Pr F'''+f_0F''+f''_0F-\left[2f'_0+K-\lambda\right]F'=0, \tag{26}$$

$$G''+f_0G'+\theta'_0F-\theta_0F'-f'_0G+\lambda G'=0, \tag{27}$$

along with the boundary condition:

$$F'(0)=0, F(0)=0, G(0)=0,$$
$$F'(\eta)\to 0, G(\eta)\to 0 \text{ as } \eta\to\infty. \tag{28}$$

It should be mentioned that for particular values of Pr, K, ε and γ, the stability of the corresponding steady flow solution $f_0(\eta)$ and $\theta_0(\eta)$ was determined by the smallest eigenvalue λ.

5. RESULTS AND DISCUSSION

The system of ordinary differential equations of equations (7)-(8) with the boundary conditions (9) is solved numerically using the bvp4c function in Matlab software. In order to test the accuracy of the present result, we have compared our results with Rosali and Ishak [7] when $\Pr=1$, $K=0$ and $K=1.2$, and $\gamma=0$ which mean there is no suction effect imposed at the boundary with different values of stretching/shrinking parameter ε. For different values of ε, the present results agree to six decimal places and that is in line with the result of Rosali and Ishak [7]. The comparison showed excellent agreement as presented in Table 1.

Table 1 Comparison of the values of $f''(0)$ for different values of ε for stretching $(\varepsilon>0)$ and shrinking $(\varepsilon<0)$ when $\Pr=1$

ε	**Present Results**		**Rosali & Ishak [7]**	
	$K=0$	$K=1.2$	$K=0$	$K=1.2$
-1.2465	0.584282	2.676432	0.554294	2.676432
-1.15	1.082310	2.651743	1.082231	2.651743
-1	1.328817	2.591239	1.328817	2.591239
-0.9	1.418077	2.537131		
-0.75	1.489298	2.436991	1.489298	2.436991
-0.6	1.507025	2.315730		
-0.5	1.495670	2.223932	1.495670	2.223932
-0.3	1.427576	2.015788		
-0.25	1.402241	1.958883	1.402241	1.958883
-0.1	1.308602	1.777080		
0	1.232588	1.646964	1.232588	1.646964
0.1	1.146561	1.509998	1.146561	1.509998
0.2	1.051130	1.366397	1.051130	1.366397
0.4	0.834072	1.060080		
0.5	0.713294	0.897720	0.713294	0.897720
1	0	0		
2	-1.887307	-2.178589	-1.887307	-2.178589
3	-4.276541	-4.798467		
5	-10.264749	-11.150137	-10.264749	-11.150137

The variations of the skin friction coefficient $f''(0)$ and the local Nusselt number $-\theta'(0)$ with stretching/shrinking parameter ε for different values of suction/injection parameter γ is shown in Figure 2 and 3, respectively. From Figure 2 and 3, it is shown that a dual solution exists for the similarity equations of equations (7)-(8) subject to the boundary condition (9). There exists a critical value ε_c with two solutions exist for $\varepsilon > \varepsilon_c$, a unique solution obtained when $\varepsilon = \varepsilon_c$ and no solutions exist for $\varepsilon < \varepsilon_c$, as shown in Figure 2 and 3. The critical values of ε_c are -2.348835, -2.389845 and -2.437, for $\gamma = 0, 0.1$ and 0.2, respectively. Table 2 shows the critical values ε_c for different γ. On the other hand, the values of $f''(0)$ and $-\theta'(0)$ for the present problem are tabulated in Tables 3 and 4.

Table 2 The critical values ε_c for some values of γ when $\Pr = 1$ and $K = 1.2$

γ	ε_c
0	-2.348835
0.1	-2.389845
0.2	-2.437

Table 3 Values of $f''(0)$ for different values of ε and γ, for stretching $(\varepsilon > 0)$ and shrinking $(\varepsilon < 0)$ when $\Pr = 1$ and $K = 1.2$

	$f''(0)$		
ε	$\gamma = 0$	$\gamma = 0.1$	$\gamma = 0.2$
-2.34	1.150900137	1.627769039	1.995295635
	(0.662286156)	(0.455557521)	(0.36020797)
-2.33	1.26525544	1.683479626	2.035207821
	(0.55302540)		
-2.32	1.350745798	1.734187464	2.072833038
	(0.472677092)		
-2.2	1.889173753	2.148684414	2.410359719
-2.1	2.137152596	2.364342699	2.597241673
-2	2.313085653	2.520128878	2.733578429
-1.8	2.538372792	2.718335459	2.904409831
-1.6	2.653192124	2.813384066	2.978991971
-1.4	2.690098066	2.833793917	2.982214859
-1.2	2.665999035	2.794991705	2.928083123
-1	2.591239275	2.706633327	2.82556621
-0.8	2.472803228	2.575334618	2.680902838

-0.6	2.315730344	2.405917688	2.498688431
-0.4	2.123834469	2.202058968	2.28245399
-0.2	1.900107747	1.966658988	2.035001852
0	1.646964429	1.702068312	1.758613683
0.2	1.366396923	1.410233504	1.455186014
0.4	1.060080009	1.092795473	1.126322451
0.6	0.729443312	0.751158138	0.773398492
0.8	0.375723001	0.386537875	0.397608396
1	0	0	0

( ) second solution

Table 4 Values of $-\theta'(0)$ for different values of ε and γ, for stretching $(\varepsilon > 0)$ and shrinking $(\varepsilon < 0)$ when $\Pr = 1$ and $K = 1.2$

	$-\theta'(0)$		
ε	$\gamma = 0$	$\gamma = 0.1$	$\gamma = 0.2$
-2.34	-2.846273194 (-4.945898633)	-2.067838194 (-9.62590335)	-1.651378021 (-26.65041223)
-2.33	-2.552346558 (-5.838610832)	-1.961620739	-1.585772172
-2.32	-2.35668347 (-6.732714624)	-1.868991071	-1.525321503
-2.2	-1.404443176	-1.211655201	-1.025200344
-2.1	-1.048707217	-0.906200636	-0.761386115
-2	-0.801508535	-0.682996631	-0.560258046
-1.8	-0.452571766	-0.357420965	-0.257693748
-1.6	-0.200458697	-0.116773431	-0.028920677
-1.4	-0.000086956	0.076786571	0.157395797
-1.2	0.167929469	0.240291438	0.316023154
-1	0.313729288	0.382884351	0.455108896
-0.8	0.443288645	0.510047771	0.579629451
-0.6	0.560429904	0.625331399	0.692850089
-0.4	0.667748079	0.731167388	0.797030914
-0.2	0.767087152	0.829296482	0.893802464
0	0.859805457	0.921008409	0.984380711

0.2	0.946933332	1.007286127	1.069697322
0.4	1.02927143	1.088896554	1.150482472
0.6	1.107454763	1.166449986	1.227319463
0.8	1.181995736	1.240440373	1.300681949
1	1.253314136	1.311273391	1.370960065

( ) second solution

In Figure 2, the first solution has a higher value of $f''(0)$ compared to the second solution for a given ε. The magnitude of $f''(0)$ increases as γ increases for both first and second solution. This is due to the suction/injection effect that increases the surface shear stress and thus increases the velocity gradient at the surface. As the γ increases, the critical values stretching/shrinking parameter ε_c for which the solution exists also increases. Consequently, the skin friction coefficient increases with the increasing of suction/injection effect parameter.

Figure 3 shows that the magnitude of $-\theta'(0)$ which represents the heat transfer rate at the surface increases as the suction/injection parameter γ increases. The first solution has a higher value of $-\theta'(0)$ as compared to the second solution. In this figure, we noticed that the second solution becomes unbounded. It is due to the fact that with the increasing of γ will increase the temperature gradient at the surface which implies in the heat transfer rate at the surface.

Figure 4 and 5 shows the effect of suction/injection parameter γ on the velocity profile and temperature profile of the shrinking case. Figure 4 has been plotted to demonstrate the effects of suction/injection γ on $f'(\eta)$ for shrinking case. It is observed that the velocity increases as γ increases for the first solution and oppositely acts for the second solution. It also can be seen that the suction effect increases the boundary layer thickness as the γ increases. Consequently, the surface shear stress increases and the skin friction coefficient increases as shown in Figure 2.

Figure 5 devotes to see the influence of the suction effect γ parameter on temperature profiles $\theta(\eta)$ for the shrinking case. From Figure 5, it is seen that the temperature increases with the increasing of γ for the second solution, while for the first solution, the temperature decreases as the γ increases. It is observed that the suction effect decreases the thermal boundary layer thickness and in turn increase the temperature gradient at the surface. As a result, as the suction/injection effect increases, the local Nusselt number on the surface also increases. Based on Figure 4 and 5, it is worth to highlight that the velocity profiles and temperature profiles satisfy the far boundary conditions asymptotically, which support the validity of numerical result and the existence of a dual solution.

As previously mentioned, the dual solution exists for a certain range of shrinking strength. Thus, a temporal stability analysis was done to verify which solution could be utilized in real-world phenomena. Stability was carried out by solving the linear eigenvalue problem in Equation (26) and Equation (27) subject to the boundary conditions Equation (28). The stable solution is identified based on the positive smallest eigenvalues λ, while the unstable solution is identified based on the negative smallest eigenvalues λ in the relation $f(\eta,\tau)=f_0(\eta)+e^{-\lambda\tau}F(\eta,\tau)$ and

$\theta(\eta,\tau)=\theta_0(\eta)+e^{-\lambda\tau}G(\eta,\tau)$. The positive values of λ gives an initial decay of disturbance which results in a stable flow, whereas negative values of λ results in the growth of disturbance and cause an unstable flow as the time pass, $\tau\to\infty$. Table 5 shows the first solution is stable and the second solution is unstable.

Table 5 Smallest eigenvalues, λ_1 for some values of ε when $\Pr=1, K=1.2$ and $\gamma=0$

ε	**First solution (Upper branch),** λ_1	**Second solution (Lower branch),** λ_1
-2.32	0.504233	-0.233151
-2.34	0.274842	-0.264783
-2.345	0.178842	-0.174538
-2.34881	0.004925	-0.001646
-2.348835	0.000000	-0.000127

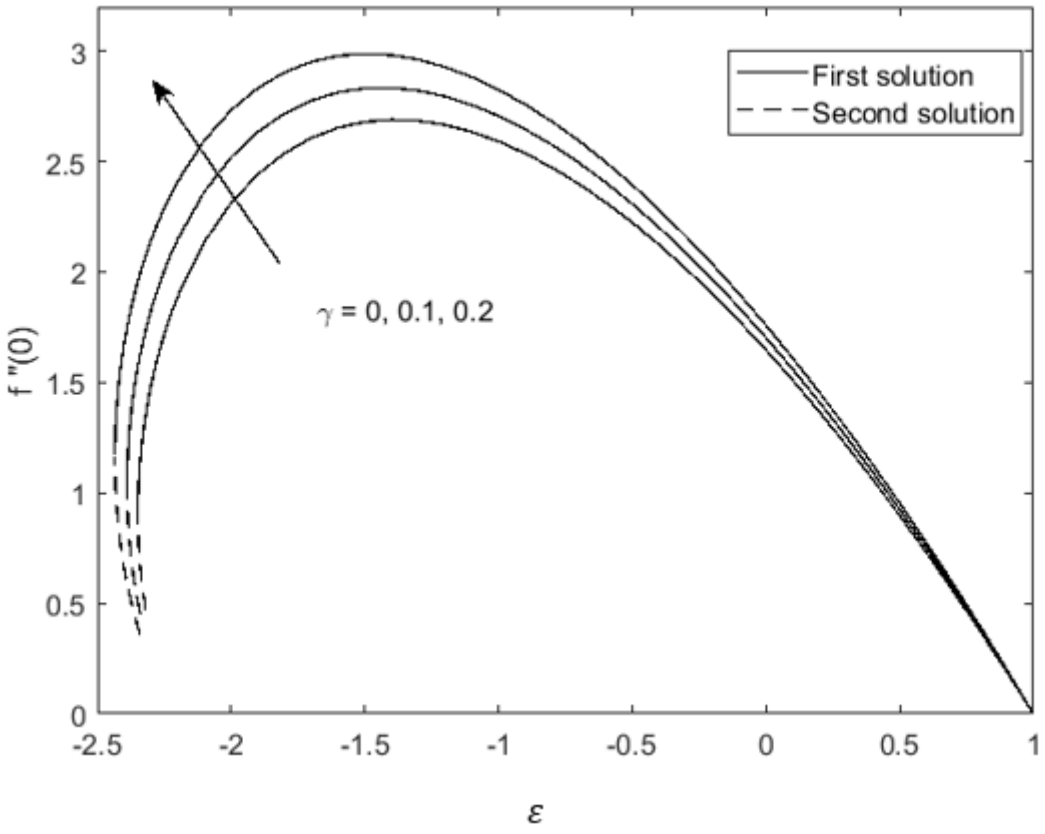

Figure 2. Variation of skin friction coefficient $f''(0)$ with ε for different values γ when $\Pr=1$ and $K=1.2$.

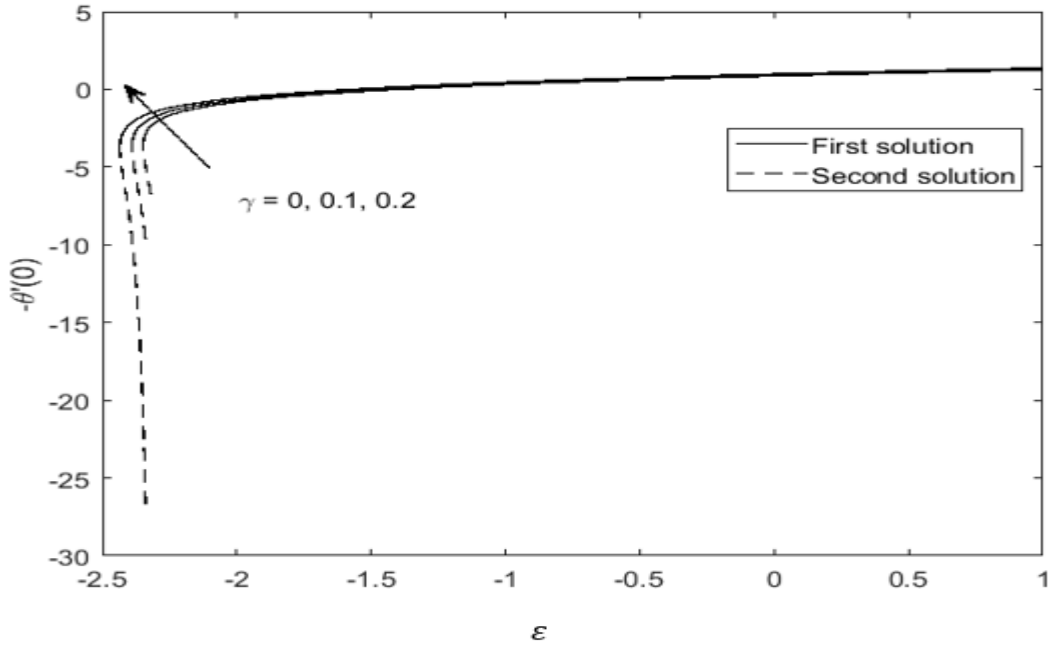

Figure 3. Variation of local Nusselt number $-\theta'(0)$ with ε for different values γ when $\Pr = 1$ and $K = 1.2$.

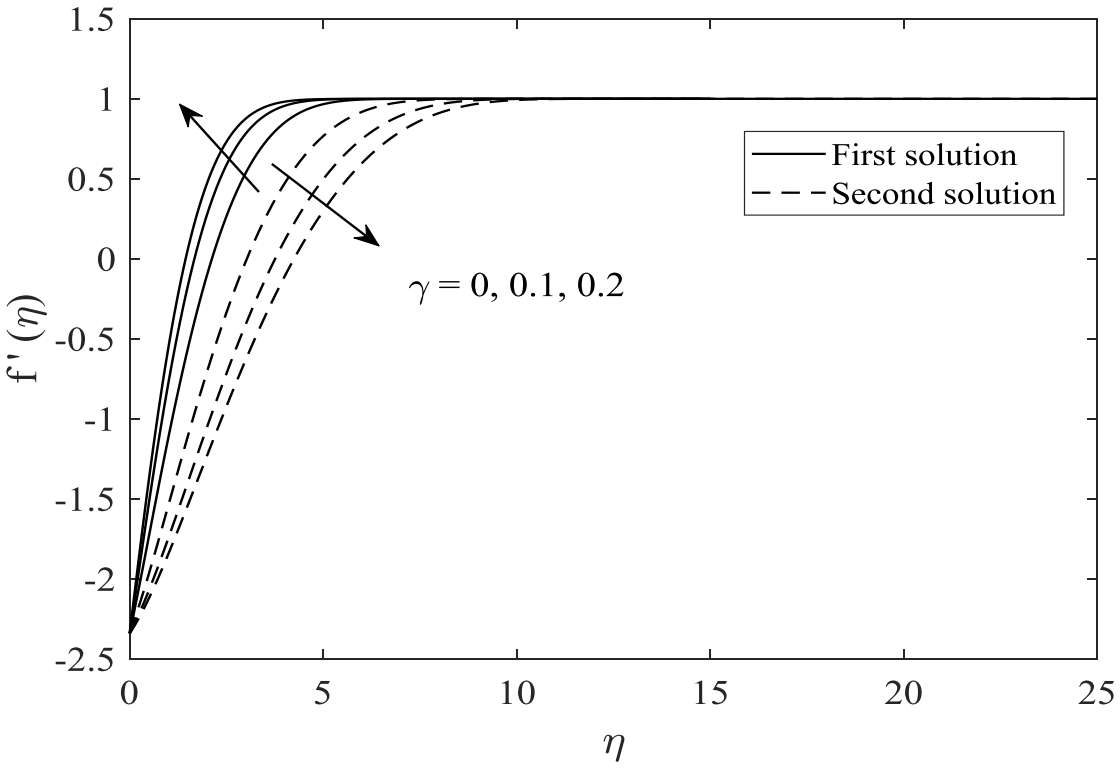

Figure 4. The velocity profiles $f'(\eta)$ for different values γ when $\Pr = 1$, $K = 1.2$ and $\varepsilon = -2.34$ (shrinking case).

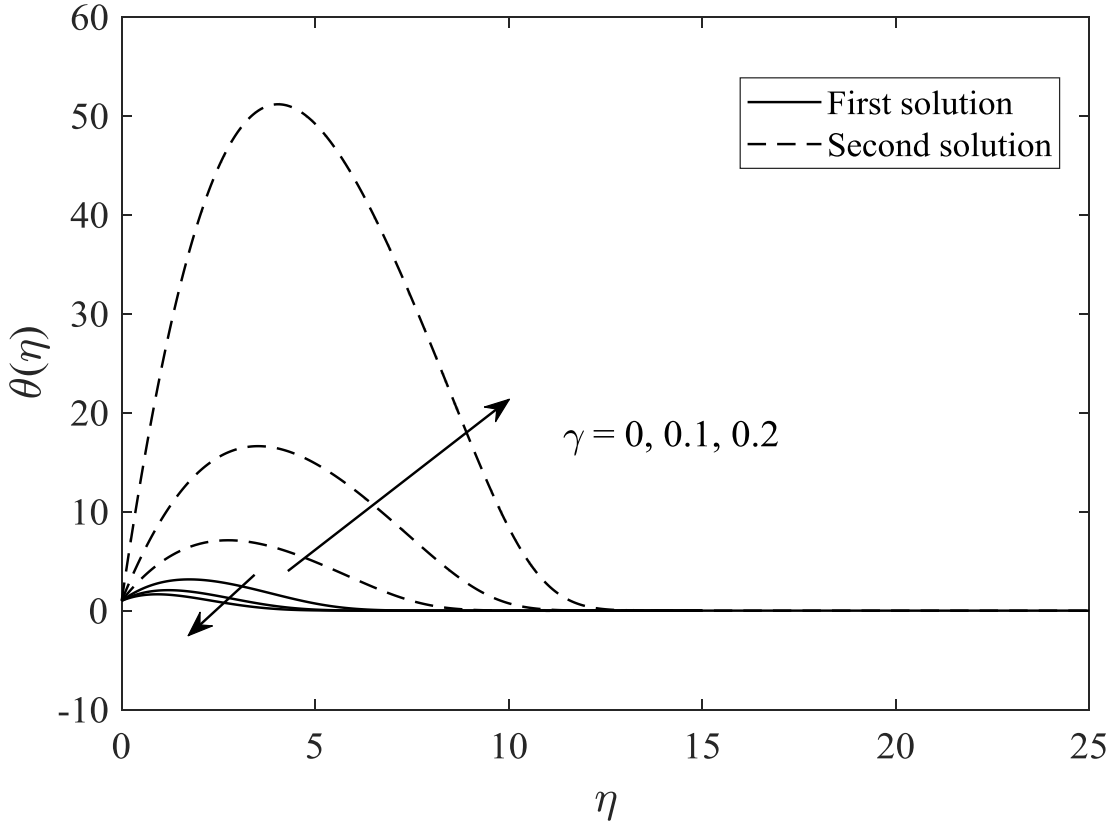

Figure 5. The temperature profiles $\theta(\eta)$ for different values γ when $\Pr = 1$, $K = 1.2$ and $\varepsilon = -2.34$ (shrinking case).

6. CONCLUSION

In this study, the problem of stagnation point flow and heat transfer over a stretching/shrinking sheet past a porous medium with suction effect is investigated. By using similarity transformation, the governing equations are reduced into ordinary differential equations and then solved numerically using the bvp4c function in Matlab software. The effects of the governing parameter, namely the suction effect on the flow and heat transfer characteristic are graphically presented and discussed. We have found that the suction effect increases the magnitude of the skin friction coefficient and the local Nusselt number. The result indicates that the velocity and temperature decrease with the suction effect at the boundary.

Then, the dual solutions exist for a certain range of shrinking case, but for stretching case, a unique solution exists. For the shrinking case, the solution exists up to the critical values of $\varepsilon_c (< 0)$ whereas, for the stretching case, the solution could be obtained for all positive values of ε. Critical values $|\varepsilon_c|$ increases as the suction parameter increases. The stability analysis was performed to prove that the first solution (upper branch) is stable while the second solution (lower branch) is unstable.

The present results are also comparable with previous studies by the previous study of specific cases. The present results are in excellent agreement with the results reported by the previous researchers.

ACKNOWLEDGEMENT

The author would like to acknowledge the support from the Fundamental Research Grant Scheme (FRGS) under a grant number of FRGS/1/2018/STG06/UNIMAP/02/3 from the Ministry of Education Malaysia.

APPENDIX

If any, the appendix should appear directly after the references without numbering, and on a new page.

REFERENCES

[1] K. Hiemenz, *Dingl Polytec. J.* **326**, 321–328 (1911).
[2] Z. Abbas, M. Sheikh & I. Pop, Journal of the Taiwan Institute of Chemical Engineers **55** (2015) 69–75.
[3] L. J. Crane, Journal of Applied Mathematics and Physics (ZAMP) **21** (1970) 645-647.
[4] P. S. Gupta & A. S. Gupta, The Canadian Journal of Chemical Engineering **55** (1977) 744 - 746.
[5] M. K. Choudhary, S. Choudhary & R. Sharma, Procedia Engineering **127** (2015) 703-710.
[6] S. Naramgari & C. Sulochana, Alexandria Engineering Journal **55**, 2 (2016) 819–827.
[7] H. Rosali & A. Ishak, AIP Conference Proceedings **1571** (2013) 949–955.
[8] A. Ishak, Y.Y. Lok, I. Pop, Chem. Eng. Comm. **197** (2010) 1417–1427.
[9] J. H. Merkin, Journal of Engineering Mathematics. **20**, 2 (1986) 171–179.
[10] P. D. Weidman, D. G. Kubitschek & A. M. J. Davis, International Journal of Engineering Science **44**, 11–12 (2006) 730–737.
[11] I. S. Awaludin, P. D. Weidman & A. Ishak, AIP Advances **6**, 4 (2016).
[12] S. Jahan, H. Sakidin, R. Nazar & I. Pop, International Journal of Mechanical Sciences, **131–132** (2017) 1073–1081.
[13] N. S. Ismail, N. Arifin, R. Nazar, N. Bachok & N. Mahiddin, International Journal of Applied Engineering Research **11**, 18 (2016) 9229–9235.